

# NASA TECHNICAL MEMORANDUM

NASA TM X-71567

NASA TM X-71567

(NASA-TM-X-71567) RADIO FREQUENCY STUDIES  
IN THE NASA LEWIS BUMPY TORUS (NASA)  
18 P HC \$3.00 CSCL 17B

N74-27623

Unclas  
63/07 43120

## RADIO FREQUENCY STUDIES IN THE NASA LEWIS BUMPY TORUS

by Glenn A. Gerdin  
Lewis Research Center  
Cleveland, Ohio



TECHNICAL PAPER presented at  
First International Conference on Plasma Science sponsored  
by the Institute of Electrical and Electronics Engineers  
Knoxville, Tennessee, May 15-17, 1974

## RADIO FREQUENCY STUDIES IN THE NASA LEWIS BUMPY TORUS

GLENN A. GERDIN\*

Lewis Research Center

## ABSTRACT

The fluctuations in potential of the plasma in the NASA Lewis Bumpy Torus are observed using capacitive probes over frequencies from 1 kHz to 25 MHz and a wide range of operating conditions. The spectra are found to differ greatly above and below a background gas pressure of  $3.4 \times 10^{-5}$  torr deuterium. Above this pressure the spectrum is dominated by the ion spoke frequency and a spectral index may be defined. Below this pressure the spectrum below 200 kHz is lower in amplitude by a factor of ten and no spectral index can be defined. At these lower pressures, fluctuations appearing to be ion spokes are observed, but have a dependence of frequency on operating conditions which is previously unreported.

## INTRODUCTION

A central problem in plasma diagnostics is to measure the plasma properties while perturbing the plasma as little as possible. A passive study of the spectrum of plasma potential fluctuations by a probe or antenna outside the plasma is a useful diagnostic tool. From Poisson's equation, these potential fluctuations arise from fluctuations in charge density of the plasma and hence carry information about the plasma dynamics. Bol (ref. 1) identified the kink instability as the driving mechanism for plasma turbulence in the Etude Stellarator, and suggested this as a driving mechanism for plasma losses. Roth (refs. 2 and 3) did a similar study in a modified Penning discharge, and observed electron and ion spokes rotating in the crossed electric and magnetic fields in the anode sheath. These spokes are associated with heating the plasma ions to high energies. The present paper extends Roth's earlier work to a modified Penning discharge in a bumpy torus geometry. This investigation had the following objectives:

- a. To see whether ion and electron spokes exist in the Bumpy Torus and whether ion spokes correlate with the ion heating process as they did in the simple mirror device.
- b. To see if any peaks exist at the ion cyclotron and ion plasma frequencies which can be used as diagnostic tools.

---

\* NASA-NRC Postdoctoral Research Associate

- c. To see whether the radio frequency spectrum reveals characteristic differences between the high and low pressure modes of operation of the **Bumpy Torus**.

#### Plasma Device and Radio Frequency Equipment

The Lewis Bumpy Torus consists of a toroidal array of twelve superconducting coils (ref. 4), see figure 1. The major diameter of the torus is 1.5 meters. The maximum magnetic field is 3.0 tesla in the coil throats and 1.2 tesla in the midplane between two coils. A 17.8 cm diameter anode ring is placed in each midplane concentric with the minor axis of the torus. These anodes are operated at a voltage up to 30 kilovolts above the grounded coils and tank. A diagram of the current-voltage characteristic of the plasma with the pressure of deuterium gas as a parameter is shown in figure 2. At constant pressure above  $2.5 \times 10^{-5}$  torr the current increases approximately as  $V^3$  until a transition voltage is reached where the current falls suddenly and then increases approximately as  $V^{3/2}$ . The first portion is referred to as the "high pressure mode" or HPM and the second portion as the "low pressure mode" or LPM.

The diagnostics on the Bumpy Torus include spectroscopic measurements of electron temperature and relative electron number density, and a charge-exchange neutral detector of the type developed by Valckx (ref. 5) to measure the ion energy distribution function. An example of such an ion energy spectrum is shown for deuterium in figure 3 along with the best fitting Maxwellian (ref. 6), where the assumption has been made that the plasma consists of only atomic ions.

The radio frequency equipment consisted of capacitive probes in two configurations. One configuration consisted, as shown in figure 4, of three probes located so as to measure the azimuthal wave number. The outputs are fed to cathode followers, then to the vertical amplifiers of a dual beam oscilloscope to obtain phase information. The frequency response of these probes was found to be flat from 1 kHz to 1 MHz. The second configuration consisted of a capacitive probe and cathode follower inserted into a 2.5 cm inner diameter re-entrant Pyrex tube. The output of the follower was connected to either a spectrum analyzer or a calibrated radio receiver. The frequency response of this system was flat from 1.5 kHz to 25 MHz. A diagram of this system is shown in figure 5. Since  $kR \ll 1$ , where  $k$  is the electro-magnetic wave number for the frequency range studied, and  $R$  is the distance between the probe and the plasma, the probes are in the near field region. Hence potential fluctuations are measured and not the radiation field. The decision to use capacitive probes was based on earlier

studies by Roth and Krawczonek (ref. 7), which indicated that, unlike Langmuir probes, no spurious sheath noise was generated around the capacitive probes up to 10 MHz.

### Results

An example of the spectrum of plasma potential fluctuations is shown in figure 6. According to a standard hydrodynamic model energy is supplied to the plasma at the low frequency end of the spectrum (refs. 2 and 3). The corresponding wavelengths are on the order of the size of the structure that drives the turbulence, approximately the diameter of the plasma. Then there is a transfer region, here between 0.9 and 5 MHz, where presumably the size of the turbulent eddies are reduced, and the frequency increased, until the turbulent energy is heavily damped in the high frequency region. In this final region of the Bumpy Torus plasma, these dissipative scale lengths are probably characterized by the ion gyroradius or the ion Debye length. Thus in this model the spectrum represents a transfer of energy from instabilities at low frequencies to thermal energy at high frequencies.

As seen in the r.f. survey on figure 6, the low frequencies are dominated by a few peaks, the waveforms of which were examined to determine the nature of the oscillation which drives the turbulence in the strong crossed dc electric and magnetic fields in the bumpy torus. Characteristic waveforms (fig. 7) strongly suggest that these peaks are similar to electron and ion spokes observed by Roth (ref. 3) in a modified Penning discharge mirror device. The mechanism driving the spoke (ref. 3) can be looked at as a positive density fluctuation in the anode sheath. This density fluctuation causes the local radial electric field in the sheath to be greater at one particular azimuthal position and causes a local increase in the  $E \times B$  drift velocity. This in turn causes a snowplow type build-up of charged particles which forms a spoke. The electron and ion spokes are decoupled and travel with different azimuthal velocities because the ions, due to finite gyroradii, spend less time in the sheath electric field than do the electrons. When the bunched electrons or ions in a given spoke pass the probe, the potential is cusped downward or upward, respectively, as is seen in the examples of waveforms from the bumpy torus in figure 7. Since the spoke is a charged bump rotating perpendicular to the  $E$  and  $B$  fields in the device, if we place probes at intervals of  $\pi/2$  radians around the minor azimuth of the torus (see fig. 4) we should see waveforms that are  $m\pi/2$  out of phase between two adjacent probes and waveform  $m\pi$  out of phase between opposite probes. Here  $m$  is an integer equal to the number of bumps co-rotating in the spoke. The results are shown for ion and electron spokes in figures 8 and 9. The electron and ion spokes are  $\pi/2$  radians apart on adjacent probes, and  $\pi$  radians apart on opposite probes as agrees with an  $m = 1$  spoke. Due to mechanical

constraints the multiple probes of figure 4 had to be placed inside the plasma. The material limitations of probes in a hot plasma restricted the plasma operating conditions to low background pressures and anode voltages for these measurements. The results on azimuthal wavenumbers using the multiple probes are only indicative of the properties of this instability at higher densities and ion energies. However, the similarity of the waveforms under a wide range of plasma conditions observed by the single probe of figure 5 is suggestive that the nature of the spokes does not change over the operating range investigated thus far.

Another result reported by Roth (ref. 3) was the increase of the ion spoke frequency,  $\nu_s$ , with the square root of the ion temperature,  $T_i$ , as given by

$$\nu_s = C T_i^{1/2} \quad (1)$$

where  $C$  is a constant of proportionality. In Roth's case (ref. 3)  $C$  is independent of pressure. Observations from the Bumpy Torus are shown for deuterium gas in figure 10(a). For a given neutral gas pressure, the ion spoke frequency increases as  $T_i^{1/2}$  (see fig. 10(b)) where the ion spokes were identified as having a waveform consisting of upward pointing cusps, and the ion temperature was measured by the charge exchange neutral analyzer.

Since the individual  $C$ 's in figure 10(a) appeared to be pressure dependent,  $C$  is plotted versus total background pressure in figure 11. For pressures below  $3.4 \times 10^{-5}$  torr,  $C$  increases with pressure as the 0.6 power and all these data are in the LPM. Above  $3.4 \times 10^{-5}$  torr  $C$  is independent of pressure in the LPM and only slightly dependent on pressure in the HPM. The dependence of  $C$  on pressure in this low pressure regime is different from the result of Roth (ref. 3) who found  $C$  to be independent of pressure over this same pressure range and 1.3 times the LPM values of  $C$  reported here at pressures above  $3.4 \times 10^{-5}$  torr.

Spectra of plasma potential fluctuations are shown in figures 6, 12(a), and 12(b). The shape of these may be grouped into the same three categories discussed in connection with the dependence of ion spoke frequency on  $T_i^{1/2}$ ; the HPM, the LPM at pressures above  $3.4 \times 10^{-5}$  torr of deuterium; and the LPM below  $3.4 \times 10^{-5}$  torr of deuterium. This pressure

boundary,  $p_b$ , of the LPM is the same as that between the two dependencies of  $C$  on pressure in figure 11.

As can be seen from the examples in figures 6 and 12, the spectra at pressures above  $p_b$  have a fairly flat band of low frequency fluctuations extending to about 200 kHz dominated by the ion spoke frequency. There is then a portion of intermediate or transfer frequencies, from about 0.8 to 4 MHz, where the amplitude of potential fluctuations falls off as a power law in frequency:

$$\phi_v = \alpha v^{-n} \quad (4)$$

where  $n$  is referred to as the spectral index and  $\alpha$  is a constant. The high frequency noise then starts at about four megahertz which would correspond to the cyclotron frequency for molecular deuterium ions although these oscillations have not been identified as such.

The lower pressure conditions,  $p \ll p_b$ , in figure 12(a) are characterized by a much lower level of plasma turbulence in the low frequency region, about a factor of ten in amplitude in the example shown. There is also a relatively small amount of energy in the ion spoke compared with lower frequency fluctuations, in contrast to the dominance of the ion spoke frequency in the LPM spectrum at pressures above  $p_b$  in figure 6. Because of the existence of peaks throughout the spectrum no spectral index could be defined for this group.

The spectral indices,  $n$ , measured at pressures above  $p_b$  are shown in a scatter plot in figure 13. The mean of these data is +2.63 and as can be seen from the figure the scatter is much greater than a typical error bar. A theory by F. F. Chen (ref. 8) based on dimensional analysis predicts a value of +2.5. Although these experimental results differ, this does not necessarily contradict Chen's theory since to apply it  $v$  must be assumed to be directly proportional to  $k$  in this region of the spectrum.

## DISCUSSION

The r.f. surveys were made under three different sets of operating conditions. These conditions are the HPM, the LPM above a certain boundary pressure,  $p_b$ , and the LPM below this boundary pressure. These operating conditions are defined by the current voltage characteristics of figure 2 and  $p_b$ .

The r.f. surveys were analyzed on the basis of the location of the ion spoke in the r.f. spectrum as a function of ion temperature and background pressure, of the power level of plasma potential fluctuations below the ion spoke frequency relative to input power, and of the presence of a spectral index. The results of this analysis are summarized in table I.

As can be seen from table I, the sets of operating conditions having the most similar r.f. spectral characteristics are the HPM and LPM above  $p_b$ . This is unexpected since they obey different power laws in their respective current-voltage characteristics. From Poisson's equation, the spectra of plasma potential fluctuations represent fluctuations in charge density and hence plasma particle dynamics. Hence, it would appear that plasma dynamics are more sensitive to background pressure than to the current-voltage power law.

TABLE I SPECTRAL CHARACTERISTICS IN EACH  
REGION OF OPERATING CONDITIONS

Functional relationship	Quantity	HPM	LPM $p > p_b$	LPM $p < p_b$
$I_p = \alpha V_A^q$	$q$	3	3/2	3/2
Ion spoke frequency	$\nu_s$	$C T_i^{1/2}$	$C T_i^{1/2}$	$C T_i^{1/2}$
$C$ as $p^x$	$x$	$< 0.6$	0	0.6
$C$ value	---	$\geq 5 \times 10^3$ Hz (eV) <sup>1/2</sup>	$4.55 \times 10^3$ Hz (eV) <sup>1/2</sup>	$< 2.75 \times 10^3$ Hz (eV) <sup>1/2</sup>
Low frequency $\frac{\phi_v^2}{I_p V_A}$	---	0.34	1	0.062
Spectral index	no	yes	yes	no

where  $p_b = 3.4 \times 10^{-5}$  torr in deuterium at a magnetic midplane field of 1.0 tesla.



## REFERENCES

1. K. Bol, "Density Fluctuations in the Etude Stellarator," Phys. Fluids, vol. 7, pp. 1855-1863, Nov. 1964.
2. J. R. Roth, "Experimental Study of Spectral Index, Mode Coupling, and Energy Cascading in a Turbulent, Hot-Ion Plasma," Phys. Fluids, vol. 14, pp. 2193-2202, Oct. 1973.
3. J. R. Roth, "Origin of Hot Ions Observed in a Modified Penning Discharge," Phys. Fluids, vol. 16, pp. 231-236, Feb. 1973.  
J. R. Roth, "Hot Ion Production in a Modified Penning Discharge," IEEE Trans. Plasma Sci., vol. PS-1, pp. 34-45, Mar. 1973.
4. J. R. Roth, A. D. Holmes, T. A. Keller, and W. M. Krawczonek, "A 12-Coil Superconducting "Bumpy Torus" Magnet Facility for Plasma Research," in Proc. 1972 Applied Superconductivity Conf., pp. 361-366, May 1972.
5. F. P. G. Valckx, "Electrostatic Analyzer for the Detection of Fast Neutral Particles," National Aeronautics and Space Administration, Tech. Trans. TT F-11, 458, June 1964.
6. J. R. Roth, "Energy Distribution Functions of Kilovolt Ions in a Modified Penning Discharge," Plasma Phys. vol. 15, pp. 995-1005, Oct. 1973.
7. J. R. Roth, and W. M. Krawczonek, "Paired Comparison Tests of the Relative Signal Detected by Capacitive and Floating Langmuir Probes in Turbulent Plasma from 0.2 to 10 MHz," Rev. of Scien. Instru., vol. 42, pp. 589-594, May 1972.
8. F. E. Chen, "Spectrum of Low- $\beta$  Plasma Turbulence," Phys. Rev. Letters, vol. 15, pp. 381-383, Aug. 30, 1965.

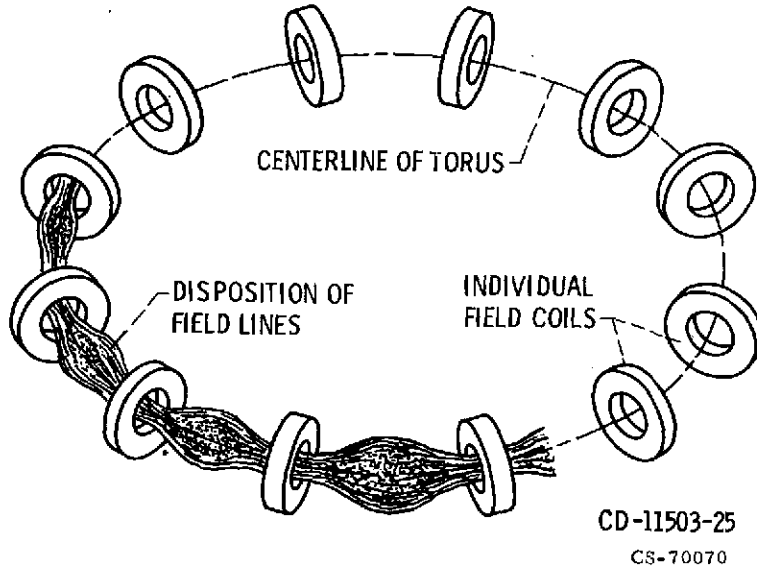


Figure 1. - Schematic drawing of the bumpy torus magnetic confinement geometry.

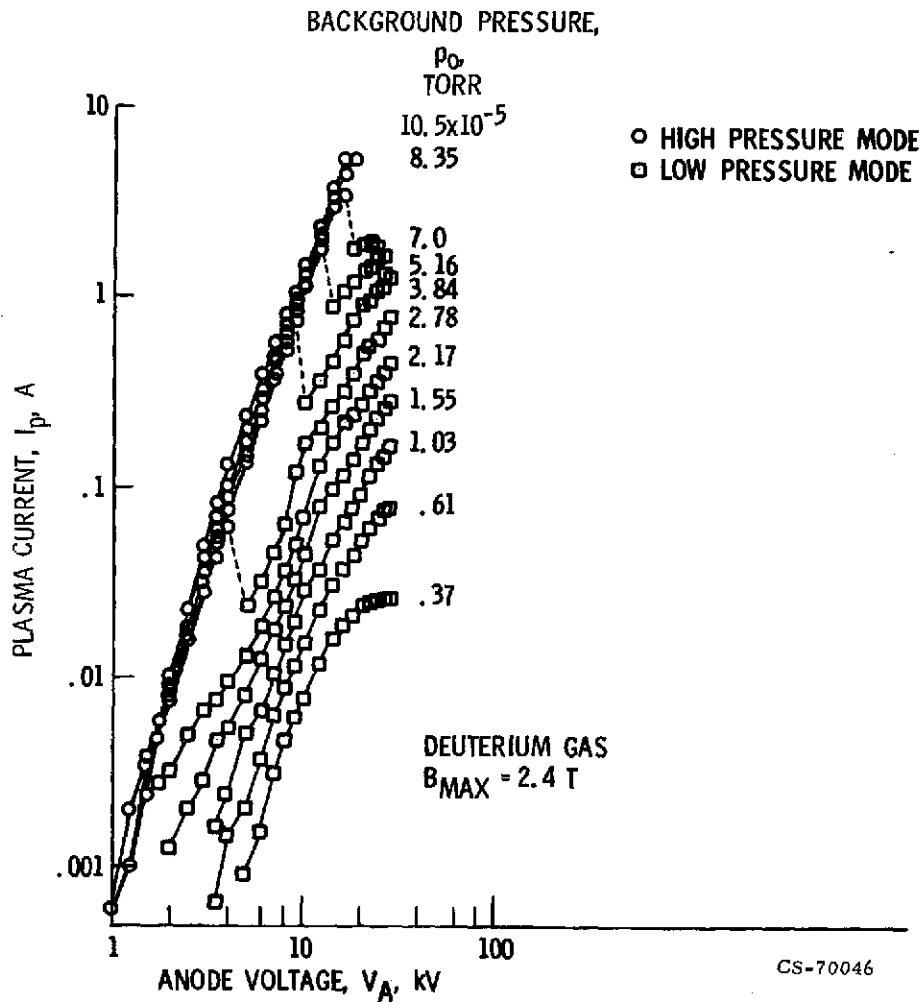
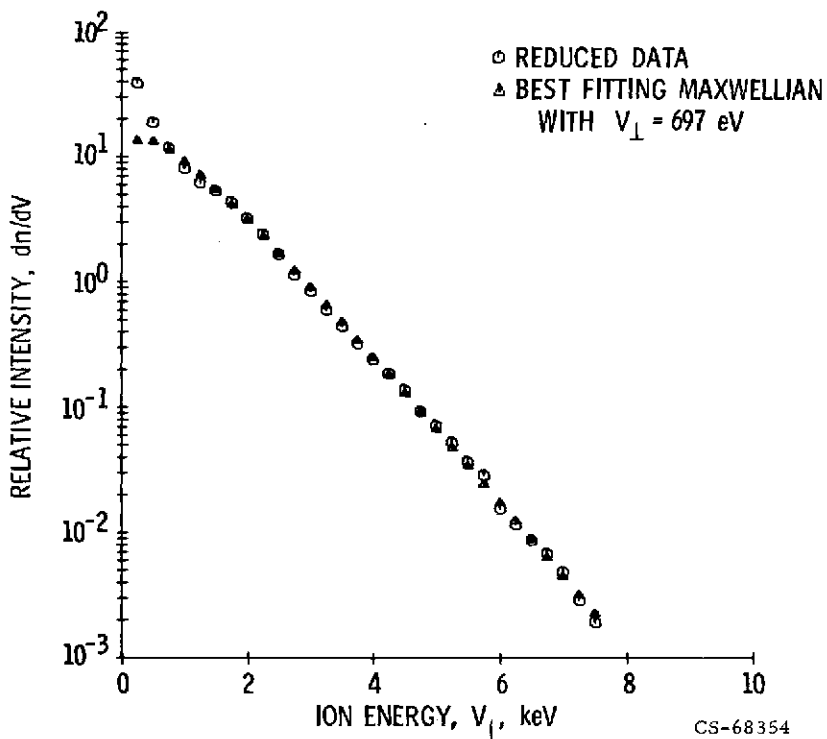


Figure 2. - Current voltage characteristic for the Lewis Bumpy Torus with a maximum magnetic field of 2.4 tesla.



(a) MAXWELLIAN DISTRIBUTION, ANODE VOLTAGE  $V_A = 8 \text{ kV}$ .

Figure 3. - An example of the ion energy spectrum in the Bumpy Torus with deuterium gas and a magnetic field maximum of 2.4 tesla. The Maxwellian fit assumes only  $D^+$  ions are sampled.

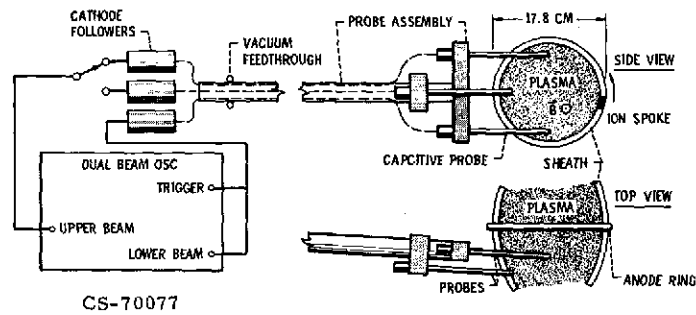


Figure 4. - Azimuthal wave number measurement apparatus.

F-8003

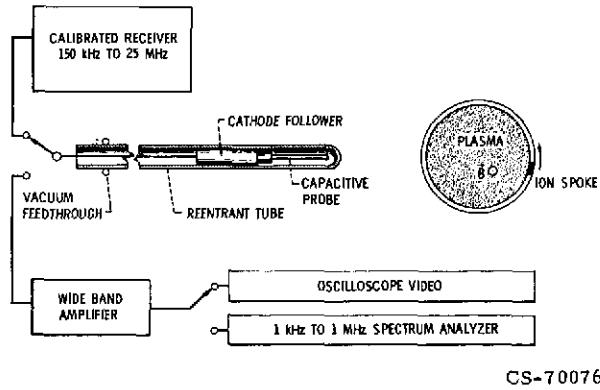


Figure 5. - R. F. survey measurement apparatus.

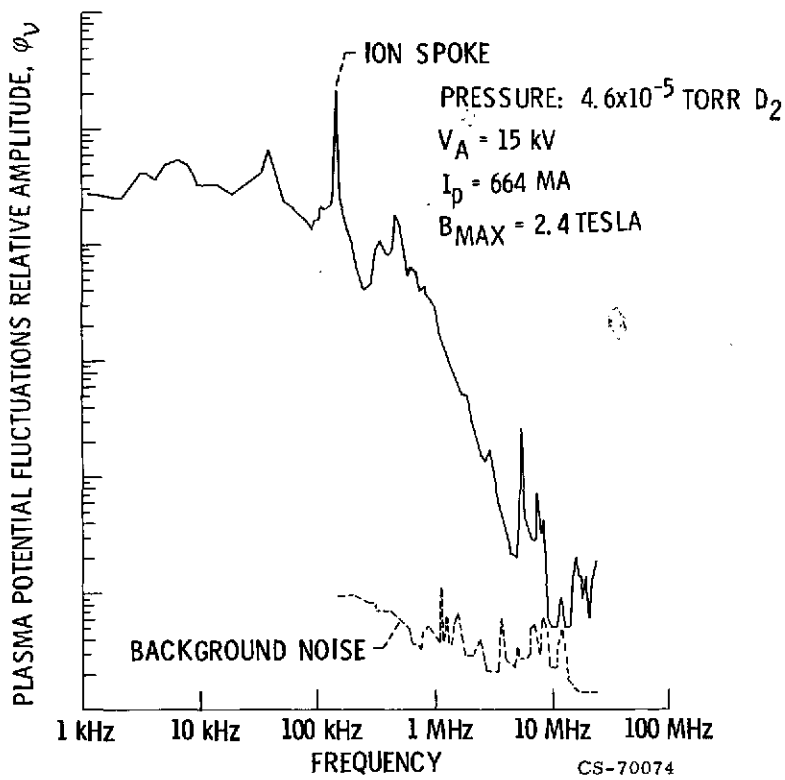
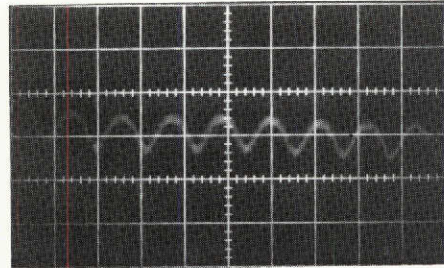
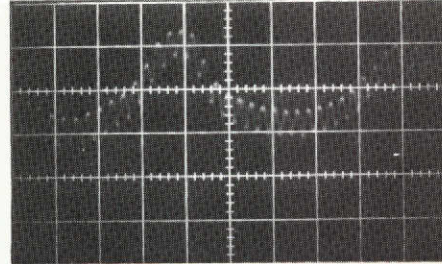


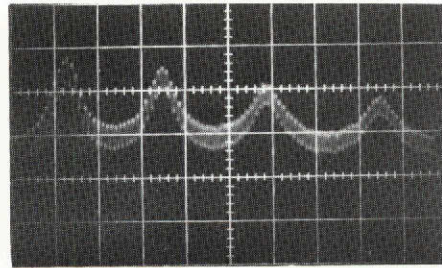
Figure 6. - An example of the fluctuations of plasma potential in the LPM, where  $\rho > \rho_D$ .



ELECTRON SPOKE,  
0.5  $\mu$ SEC/CM,  $\approx$ 1.8 MHz



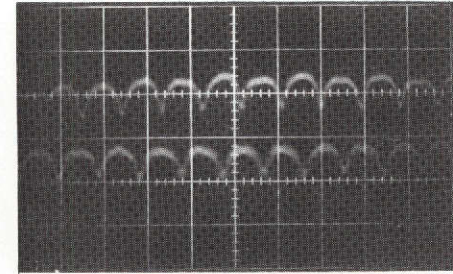
ELECTRON & ION SPOKE MODULATION,  
2.0  $\mu$ S/CM,  $\approx$ 1.8 MHz, 95 kHz



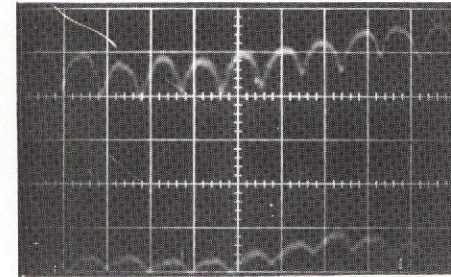
ION SPOKE,  
5  $\mu$ S/CM,  $\approx$ 95 kHz

CS-70051

Figure 7. - Electrostatic potential waveform from a single capacitive probe in the arrangement of figure 5. The operating conditions were: anode voltage  $V_A = 18$  kV; anode current  $I_A = 76$  ma; tank pressure  $p = 5.3 \times 10^{-5}$  torr of deuterium; and a maximum magnetic field of 1.44 tesla.

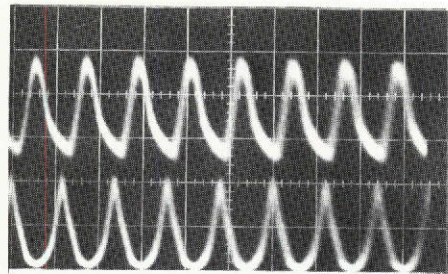


(a) PROBES SEPARATED BY  $180^\circ$ .

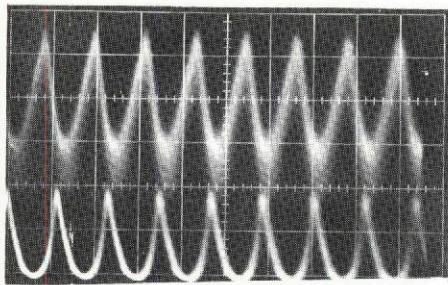


(b) PROBES SEPARATED BY  $90^\circ$ . CS-70050

Figure 8. - Same operating conditions as figure 7; electrostatic potential waveforms from two capacitive probes with indicated angular separation in minor azimuth. Both show the electron spoke with time base 0.5  $\mu$ s/cm. Negative potential cusps and phase differences of the waveforms are consistent with an  $m = 1$  electron spoke.



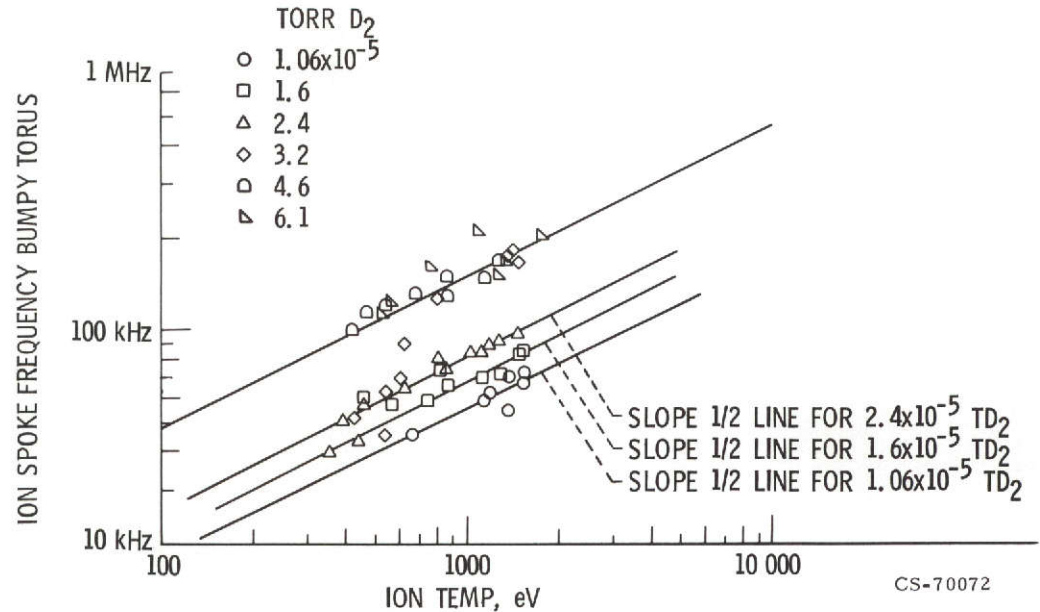
(a) PROBE SEPARATION  $180^\circ$ .



(b) PROBE SEPARATION  $90^\circ$ .

CS-70049

Figure 9. - Electrostatic potential waveforms from two capacitive probes with indicated separation in minor azimuth. Upward pointing cusps and phase changes are consistent with an  $m = 1$  ion spoke rotating in the same sense as the electron spoke of figure 8. Time base  $20 \mu\text{s}/\text{cm}$ ; both show ion spoke with frequency  $\approx 42 \text{ kHz}$  for operating conditions anode voltage  $V_A = 5.0 \text{ kV}$ ; background pressure  $2 \times 10^{-5}$  torr of deuterium; maximum magnetic field  $B_{\text{max}} = 2.4$ .

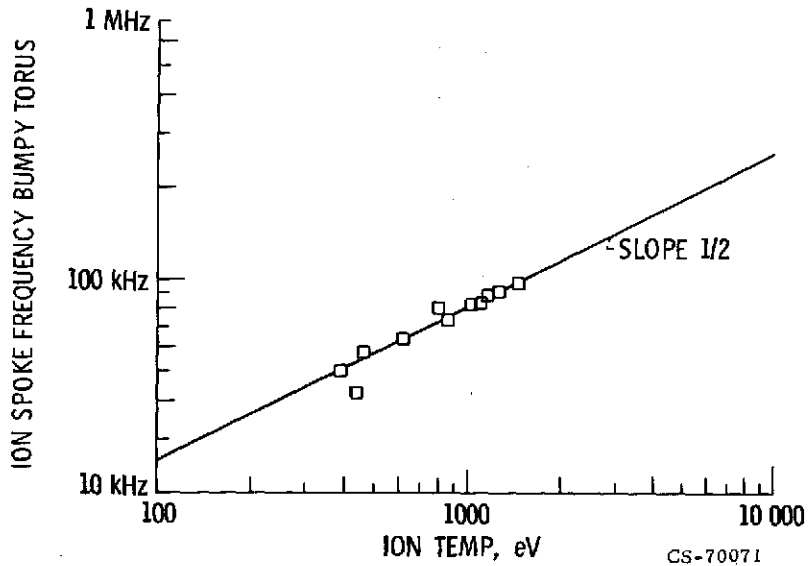


CS-70072

(a) AT CONSTANT MAGNETIC FIELD OF 2.4 TESLA. THE LINES HAVE A SLOPE OF ONE-HALF AND THE DATA AT A GIVEN PRESSURE TEND TO FALL ALONG ONE OF THESE LINES.

Figure 10. - Ion spoke frequency vs. ion temperature.

71



(b) AT CONSTANT MAGNETIC FIELD AND BACKGROUND PRESSURE OF  $2.4 \times 10^{-5}$  TORR DEUTERIUM.

Figure 10. - Concluded.

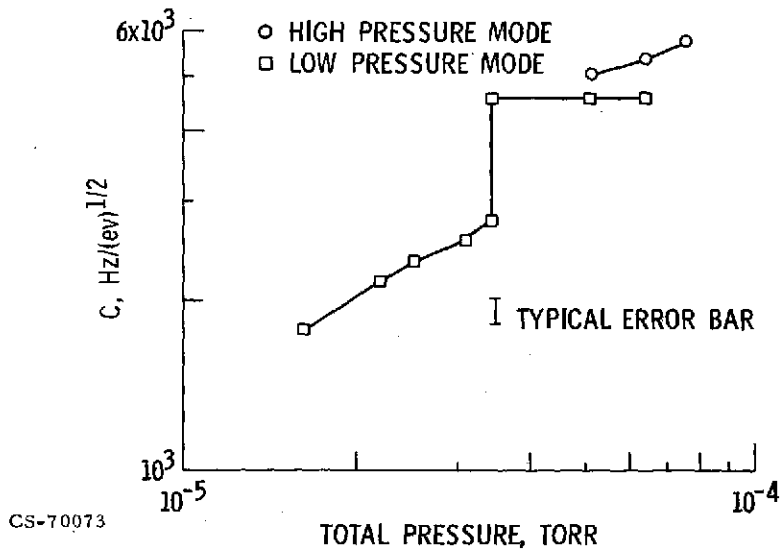
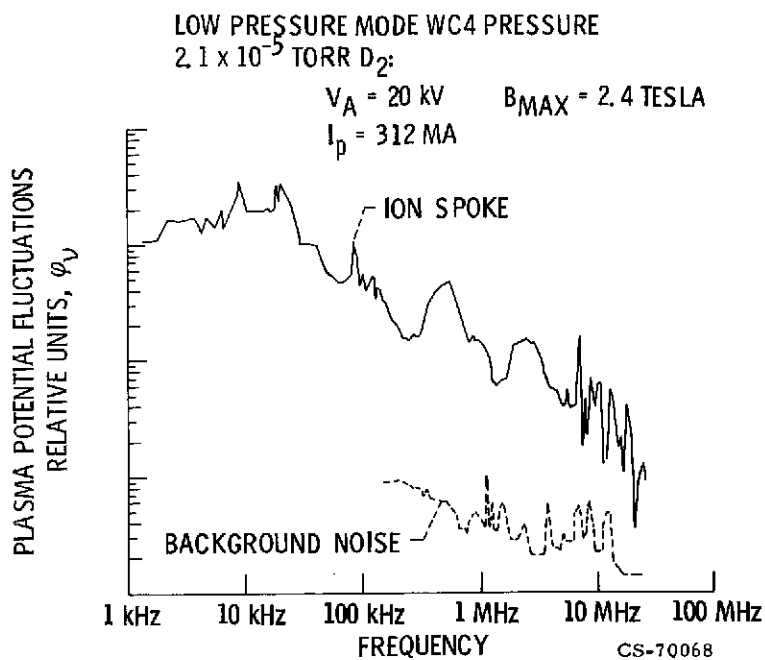


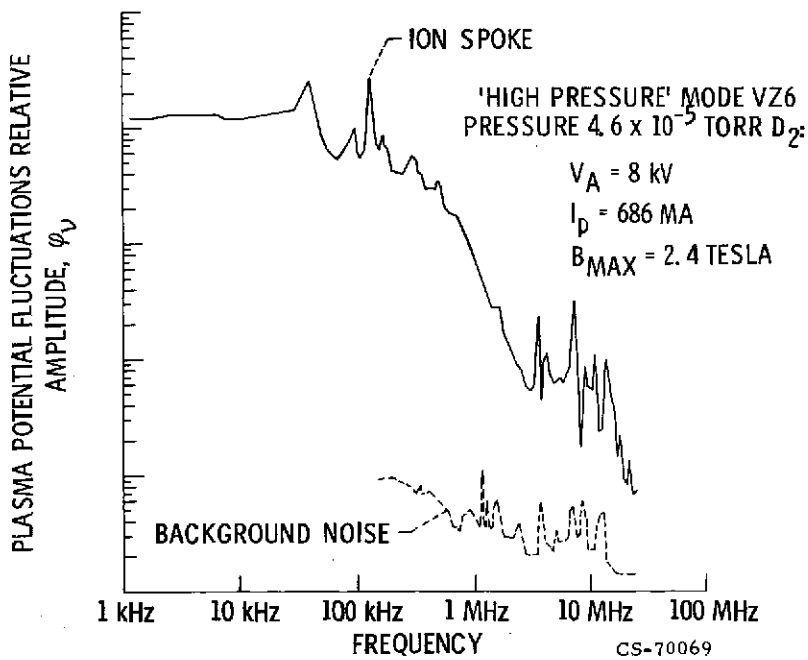
Figure 11. - C vs. pressure, where  $v_s = C T_i^{1/2}$ .





(a) AT  $P < P_b$  IN LPM.

Figure 12. - The plasma potential fluctuation spectrum.



(b) IN THE HPM.

Figure 12. - Concluded.

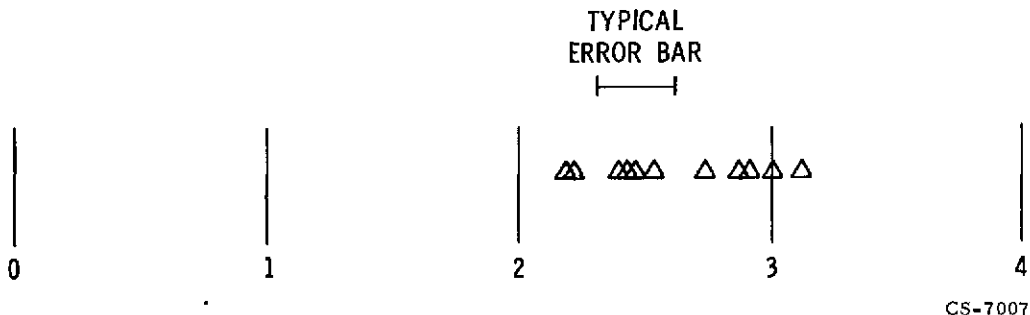


Figure 13. - Scatter plot of spectral index.

CS-70075

E-8003